Rapid Report

Malignant hyperthermia mutation Arg615Cys in the porcine ryanodine receptor alters voltage dependence of Ca^{2+} release

B. Dietze, J. Henke*, H. M. Eichinger†, F. Lehmann-Horn and W. Melzer

*Department of Applied Physiology, University of Ulm, Albert-Einstein-Allee 11, D-89069 Ulm, †Experimental Centre Thalhausen, TU Munich, D-85402 Kranzberg and *Institute for Experimental Oncology and Therapy Research, TU Munich, D-81675 Munich, Germany*

(Received 17 April 2000; accepted after revision 9 June 2000)

1. Ca^{2+} inward current and fura-2 Ca^{2+} transients were simultaneously recorded in porcine myotubes. Myotubes from normal pigs and cells from specimens homozygous for the Arg615Cys (malignant hyperthermia) mutation of the skeletal muscle ryanodine receptor RyR1 were investigated. We addressed the question whether this mutation alters the voltage dependence of Ca^{2+} release from the sarcoplasmic reticulum.

2. The time course of the total flux of Ca^{2+} into the myoplasm was estimated. Analysis showed that the largest input Ca^{2+} flux occurred immediately after depolarization. Amplitude and time course of the Ca^{2+} flux at large depolarizations were not significantly different in the Arg615Cys myotubes.

3. Ca^{2+} release from the sarcoplasmic reticulum was activated at more negative potentials than the L-type Ca^{2+} conductance. In the controls, the potentials for half-maximal activation ($V_{½}$) were −9·0 mV and 16·5 mV, respectively.

4. In myotubes expressing the Arg615Cys mutation, Ca^{2+} release was activated at significantly lower depolarizing potentials ($V_{½} = -23{\cdot}5$ mV) than in control myotubes. In contrast, $V_{½}$ of conductance activation (13·5 mV) was not significantly different from controls.

5. The specific shift in the voltage dependence of Ca^{2+} release caused by this mutation can be well described by altering a voltage-independent reaction of the ryanodine receptor that is coupled to the voltage-dependent transitions of the L-type Ca^{2+} channel.

Malignant hyperthermia is a life-threatening pharmacogenetic hypermetabolic state that can be observed in susceptible individuals during general anaesthesia. It results from excessive Ca^{2+} release from the sarcoplasmic reticulum (SR) of skeletal muscle under the influence of volatile anaesthetics and/or depolarizing muscle relaxants (MacLennan & Phillips, 1992; Mickelson & Louis, 1996). In the majority of cases, this inherited muscle disorder is caused by point mutations of the SR Ca^{2+} release channel RyR1 (type 1 isoform of the ryanodine receptor; Jurkat-Rott *et al.* 2000).

A homologue of one of the most frequently found human RyR1 mutations (Arg614Cys) is also present in pigs (Arg615Cys) causing a similar phenotype when expressed homozygously and giving rise to porcine stress syndrome (PSS). As in humans, a higher sensitivity to volatile anaesthetics and Ca^{2+} releasing agents such as caffeine was found (Iaizzo & Lehmann-Horn, 1989). Ca^{2+} release in skeletal muscle is controlled by interaction of RyR1 with the α_{1S}-subunit of the dihydropyridine (DHP) receptor that functions as a sensor of the plasma membrane voltage (Melzer *et al.* 1995). It has been reported that muscle from pigs carrying the Arg615Cys mutation responds more readily to depolarization by solutions with elevated potassium concentrations (Gallant & Donaldson, 1989; Gallant & Lentz, 1992; Gallant & Jordan, 1996). Furthermore, a decreased voltage threshold for activation of contraction has been demonstrated in myotubes from pigs with this mutation (Gallant & Jordan, 1996). These results point to an altered voltage control of SR Ca^{2+} release.

To investigate this question we studied myotubes of pigs homozygous for the Arg615Cys mutation (malignant hyperthermia-susceptible (MHS) pigs). We simultaneously monitored Ca^{2+} inward currents and fura-2 Ca^{2+} transients under voltage-clamp conditions to compare signals originating from the DHP receptor and from the Ca^{2+} release channel.

METHODS

Genetic analysis

Pietrain pigs, homozygous for the Arg615Cys mutation, and German Landrace pigs, homozygous for the wild-type, were used for the experiments. The animals were genetically tested using genomic DNA isolated from blood leucocytes. The primers MH1 (5′-GTT CCC TGT GTG TGT GCA AT-3′) and MH3 (5′-CGT GTG ACA TAG ATG AGG TTT G-3′) were used for polymerase chain reaction (PCR). Amplified DNA was subjected to restriction enzyme digestion (HhaI, Pharmacia) and agarose gel electrophoresis. Homozygous mutants showed an undigested 118 bp fragment while homozygous normal animals showed two fragments of 85 bp and 33 bp.

Cell culture

Two- to three-month-old pigs were anaesthetized and killed with barbiturate or propofol, in accordance with the regulations of the local ethics committee. Pieces of the longissimus dorsi muscle (0·5 g) were excised. The muscle samples were transferred to the laboratory in Hanks' solution (0 °C). To isolate the satellite cells (Brinkmeier *et al.* 1993), the muscle samples were cut into small pieces with fine scissors and subjected to enzymatic dissociation with gentle agitation for 60 min at 37 °C. The dissociation solution consisted of F12 medium (Gibco) containing 1·5 mg ml^{-1} collagenase (17449, Serva I), 2 mg ml^{-1} protease (P6141, Sigma Type IX), 50 μg ml^{-1} gentamicin (Biochrom) and 2 mM Hepes, pH 7·2. After filtering (pore size 50 μm), the resulting suspension was centrifuged and the pellet was resuspended in growth medium: F12 solution with 15% fetal calf serum (Gibco) and 2% chicken embryo extract (Gibco). The culture was preplated for 20 min to reduce the number of fibroblasts and the cells remaining in suspension were then seeded into culture flasks with growth medium. Four days later the cells were detached from the flask by trypsin (0·15% trypsin and 0·08% EDTA in Ca^{2+} and Mg^{2+} free phosphate buffered saline (PBS), all compounds from Biochrom) and plated on carbon and collagen coated coverslips. The next day the medium was changed to Dulbecco's modified Eagle's medium (DMEM) with 5% horse serum (both from Gibco) to induce differentiation. Most cells were measured 2 to 5 days after reduction of the serum concentration. Intermediate sized myotubules devoid of branches were selected to obtain acceptable calcium transients and voltage control. The criteria of selection were the same for the two groups of myotubes and consequently the passive electrical parameters were similar (Fig 4*A*, legend).

Solutions

The experimental solutions were made of the following components. Bathing solution was composed of (mM): 140 tetraethylammonium hydroxide (TEAOH), 135 HCl, 10 $CaCl_2$, 1 $MgCl_2$, 10 Hepes, 2·5 4-aminopyridine (4-AP), 0·1 EGTA, 0·0013 tetrodotoxin (TTX); pH 7·4. Pipette solution was (mM): 150 CsOH, 135 HCl, 0·66 $CaCl_2$ (resulting in 20 nM free Ca^{2+}), 0·5 $MgCl_2$, 10 Hepes, 5 EGTA, 5 MgATP, 5 sodium creatine phosphate, 0·2 fura-2 (pentapotassium salt), pH 7·2. In 12 experiments 400 μM fluo-3 instead of 200 μM fura-2 was used.

Current measurements and analysis

Myotubes were voltage clamped as described in Dietze *et al.* (1998). The pCLAMP 6.0 software package (Axon Instruments) and Excel (Microsoft) were used for analysis. The last 8 ms before the end of the stimulus were averaged to obtain the voltage dependence of current and fluorescence. The current–voltage relations were least-squares fitted with eqn (1):

$$I(V) = g_{\text{leak}}(V - V_{\text{leak}}) + f(V)g_{\text{Ca,max}}(V - V_{\text{Ca}}), \quad (1)$$

where

$$f(V) = \frac{1}{1 + \exp((V_{½} - V)/k)}, \quad (2)$$

g_{leak} and V_{leak} are conductance and reversal potential of a leak component, respectively, and $g_{\text{Ca,max}}$ and V_{Ca} are maximal conductance and reversal potential, respectively, of the L-type Ca^{2+} current. $f(V)$ represents voltage dependence of activation; $V_{½}$ and k, voltage of half-maximal activation and voltage sensitivity, respectively.

Fluorescence measurements

Coverslips carrying the myotubes were mounted in a Plexiglas chamber on an inverted epifluorescence microscope (IMT-2, Olympus) equipped with a microscope photometer (SF, Zeiss, photomultiplier tube: R 928, Hamamatsu). Fura-2 fluorescence was measured at the emission wavelength of 510 nm. Excitation wavelengths of 380 nm (for Ca^{2+} signals) and 358 nm (isosbestic point) were used. In the case of the fluo-3 measurements the excitation and emission wavelengths were 485 and 530 nm, respectively. $\Delta F/F$, the depolarization-induced fluorescence change divided by the resting fluorescence at the same wavelength, was used to determine the voltage dependence of the release process.

All experiments were carried out at room temperature (20–23 °C). Mean data are presented and plotted as means ± S.E.M. (n = number of cells). Student's t test was used to test for significant differences of mean values ($P = 0·05$).

RESULTS

To investigate the dynamics of the flux of Ca^{2+} entering the myoplasm during a depolarization in porcine myotubes, we determined the time derivative of an approximate estimate of the total myoplasmic Ca^{2+}. The fluorescence ratio R, i.e. the fluorescence signal at 380 nm excitation divided by the resting fluorescence at 358 nm excitation (recorded 1 s before each voltage-clamp pulse) was converted to the concentration of free Ca^{2+}. In this step, correction of non-instantaneous binding of Ca^{2+} by fura-2 was made (see Klein *et al.* 1988, Dietze *et al.* 1998). The result was used to calculate the occupancy of the intracellular binding components that are thought to capture most of the released Ca^{2+}. The EGTA diffusing into the cell from the pipette provided the main Ca^{2+} buffer component under our conditions and its kinetic parameters were therefore dominant for the analysis result. Calculations using *in vitro* rate constants of EGTA, determined by Smith *et al.* (1984), produced a transient negative phase after termination of the pulse (Fig. 1*A*). A comparable phase could not be detected in the corresponding free Ca^{2+} transients (not shown). The most effective way to reduce the undershoot and to ensure that the flux returns close to baseline values after repolarization, was to increase both rate constants (Fig. 1*B*; see legend for further details).

Even though flux calculated in this way (Fig. 1) can only be a rather crude estimate due to the uncertainties in the kinetic constants and concentrations, the following conclusions proved to be independent of the choice of constants. The input flux reaches a maximum at the beginning of the pulse and declines during the pulse. It, therefore resembles estimates in other vertebrate muscle cells that show a higher rate of Ca^{2+} mobilization early during depolarization (e.g. Melzer *et al.* 1987; Shirokova *et al.* 1996; Dietze *et al.* 1998). The flux drops almost instantaneously at the time of repolarization. Neither time course nor amplitude differed significantly in the MHS myotubes compared with controls as judged by comparing the following signal parameters of the two groups of cells: peak value (PV), value at the end of pulse (EV), time from pulse onset to peak (TTP) and half time of decay (HTD) during the pulse (see legend of Fig. 1).

Due to the involvement of time derivatives the flux calculations are sensitive to noise. Because the limited lifetime of the myotubes in the whole-cell configuration did not allow extensive signal averaging the input flux analysis had to be restricted to one voltage (+20 mV). To investigate the voltage dependence of Ca^{2+} release we, therefore, used the

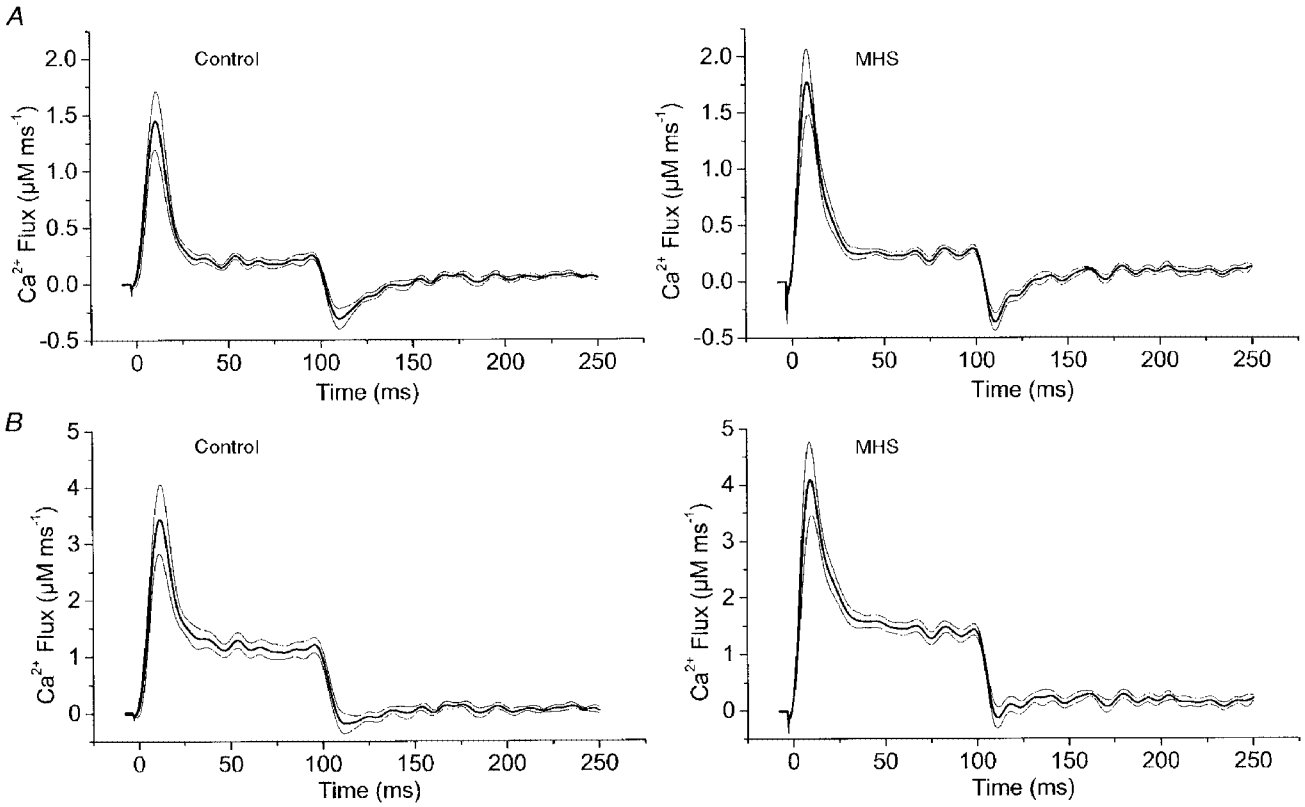

Figure 1. Determination of the time course of Ca^{2+}-input flux

An estimate of the total flux of Ca^{2+} into the myoplasm (Ca^{2+}-input flux) was obtained by the general procedure of Baylor *et al.* (1983). The Ca^{2+} flux was calculated (for equations see Baylor *et al.* 1983 and Brum *et al.* 1988) considering fura-2 (0·2 mM), EGTA (5 mM) and troponin C (0·24 mM of fast Ca^{2+}-specific T sites and 0·24 mM of slow Ca^{2+}–Mg^{+} sites with parvalbumin-type behaviour, P-sites; rate constants from Baylor & Hollingworth, 1998). The parameter values used were as follows: T sites: $k_{on,Ca,T} = 88{\cdot}5\ \mu M^{-1}\ s^{-1}$, $k_{off,Ca,T} = 115\ s^{-1}$; P sites: $k_{on,Ca,P} = 41{\cdot}7\ \mu M^{-1}\ s^{-1}$, $k_{off,Ca,P} = 0{\cdot}5\ s^{-1}$; $k_{on,Mg,P} = 0{\cdot}033\ \mu M^{-1}\ s^{-1}$, $k_{off,Mg,P} = 3\ s^{-1}$. For EGTA we chose the rate constants of Smith *et al.* (1984): $k_{on,Ca,EGTA} = 1{\cdot}5\ \mu M^{-1}\ s^{-1}$, $k_{off,Ca,EGTA} = 0{\cdot}3\ s^{-1}$. This set of parameters produced a transient phase of negative flux after repolarization (*A*). To reduce this phase we had to increase the published *in vitro* rate constants of EGTA by a factor of 10 at constant K_D (*B*). This adjustment did not alter the general shape of the signals during the depolarization. For comparison of amplitude and time course we determined the four parameters PV, EV, TTP and HTD (see text). In *A*, the values were $1{\cdot}99 \pm 0{\cdot}25\ \mu M\ ms^{-1}$, $0{\cdot}27 \pm 0{\cdot}03\ \mu M\ ms^{-1}$, $9{\cdot}7 \pm 1{\cdot}0$ ms and $15{\cdot}3 \pm 1{\cdot}2$ ms for MHS *versus* $1{\cdot}67 \pm 0{\cdot}24\ \mu M\ ms^{-1}$, $0{\cdot}22 \pm 0{\cdot}03\ \mu M\ ms^{-1}$, $11{\cdot}5 \pm 1{\cdot}5$ ms and $16{\cdot}8 \pm 1{\cdot}5$ ms for control. In *B* values were $4{\cdot}6 \pm 0{\cdot}6\ \mu M\ ms^{-1}$, $1{\cdot}4 \pm 0{\cdot}1\ \mu M\ ms^{-1}$, $10{\cdot}5 \pm 1{\cdot}1$ ms and $16{\cdot}4 \pm 1{\cdot}3$ ms for MHS *versus* $3{\cdot}9 \pm 0{\cdot}6\ \mu M\ ms^{-1}$, $1{\cdot}1 \pm 0{\cdot}1\ \mu M\ ms^{-1}$, $12{\cdot}3 \pm 1{\cdot}5$ ms and $17{\cdot}6 \pm 1{\cdot}5$ ms for control. They showed no significant difference. Mean results of 10 control and 11 MHS measurements. Thin lines indicate S.E.M.

Ca^{2+}-dependent fluorescence transients. Figure 2 shows an example experiment on a myotube from a normal pig. Simultaneously with fluorescence (Fig. 2*B*), we measured the activation of the slow Ca^{2+} inward current (L-type current, Fig. 2*A*). Depolarizing pulses of 100 ms duration were applied. The pulses were separated by intervals of 20 s to allow for recovery from the previous activation. Figure 2*C* and *E* show the voltage dependence of both signals.

It can be noticed that the Ca^{2+} signal (Fig. 2*E*) is activated at more negative voltages ($V_{½} = -8{\cdot}2$ mV) than the L-type conductance (Fig. 2*D*; $V_{½} = 17{\cdot}0$ mV). Consequently, at 0 mV the inward current is just slightly above threshold, while the Ca^{2+} signal has already reached about 80% of its maximal value. At large depolarizations, a decline of the Ca^{2+} signal amplitude can be noticed. Most of the decline appeared to be due to a run down of Ca^{2+} release as could be shown by repeating a test pulse to +20 mV at the end of the sequence (open symbol).

Figure 3 shows Ca^{2+} currents and fura-2 Ca^{2+} signals simultaneously measured at different potentials in a single MHS myotube. Again, Ca^{2+} signals became activated at more negative potentials than Ca^{2+} conductance (Fig. 3*D* and *E*). However, the difference between $V_{½}$ values of Ca^{2+} signal and conductance is clearly larger than in the experiment of Fig. 2 (41·5 *versus* 25·2 mV). A Ca^{2+} signal was already measured at −30 mV (Fig. 3*B*) whereas the control myotube of Fig. 2*B* showed no response at this potential.

Figure 4*A* shows the average results of 9 control and 19 MHS myotubes. Apart from a modest difference in the steepness of the Ca^{2+} conductance activation ($k = 6{\cdot}1 \pm 0{\cdot}2$ *versus* $4{\cdot}9 \pm 0{\cdot}4$ mV in controls, $P = 5{\cdot}4 \times 10^{-3}$), no significant differences were found in the current measurements between the two groups of cells. Also the passive electrical characteristics were very similar (see legend of Fig. 4).

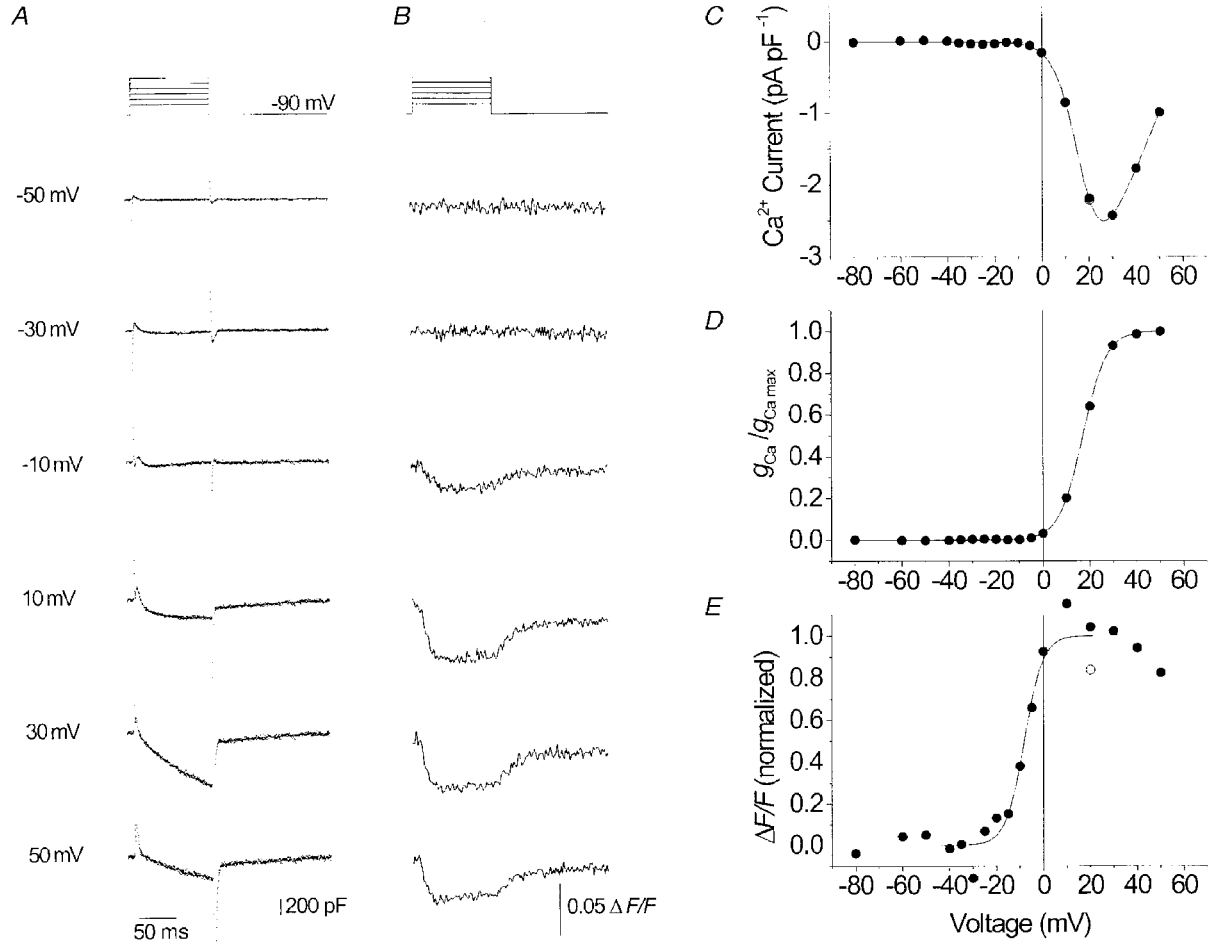

Figure 2. Ca^{2+} current and Ca^{2+} transients in a normal porcine myotube

L-type Ca^{2+} inward currents (*A*) and fura-2 fluorescence signals (*B*) recorded at voltage-clamp steps from −90 mV to values between −50 and +50 mV. *C*, current–voltage relation. *D*, voltage dependence of Ca^{2+} conductance activation. *E*, voltage dependence of activation of the Ca^{2+} signal. The free calcium concentration determined prior to pulse activation (resting $[Ca^{2+}]$) was 16 nM, the increase ($\Delta[Ca^{2+}]$) at +20 mV was 10 nM. The best fit parameter values (see Methods, eqns (1) and (2)) were as follows, current: $g_{Ca,max} = 80{\cdot}8$ pS pF^{-1}, $V_{Ca} = 62{\cdot}2$ mV, $V_{½} = 17{\cdot}0$ mV, $k = 5{\cdot}1$ mV. Fluorescence: $V_{½} = -8{\cdot}2$ mV, $k = 4{\cdot}0$ mV.

On the other hand, the MHS myotubes showed a 14·5 mV shift of the activation curve for Ca^{2+} release ($V_{½} = -23·5 \pm 1·2$ *versus* $-9·0 \pm 2·4$ mV in controls). Student's t test indicated a highly significant ($P = 2·1 \times 10^{-6}$) difference between the two $V_{½}$ values.

Thus in conclusion, the mutation caused a shift of Ca^{2+} release activation to more negative potentials. The voltage dependence of the L-type Ca^{2+} conductance showed no comparable alteration and the maximum Ca^{2+} release rate and its time course at large depolarization appeared to be unchanged.

DISCUSSION

Only a small number of investigations on cultured myocytes is available in which the voltage-dependent activation of L-type Ca^{2+} current and intracellular Ca^{2+} signals have been directly compared (Garcia & Beam, 1994; Strube *et al.* 1996; Dietze *et al.* 1998). As described in these investigations, in the porcine cells studied here, Ca^{2+} release from the SR appeared at more negative potentials than the Ca^{2+} inward current. This is compatible with sequential reaction schemes for a dual control mechanism of the DHP receptor in which transitions between closed states – involved in gating the Ca^{2+} release channel of the SR – occur before the transition to the open state that allows Ca^{2+} entry from the extracellular space (Garcia *et al.* 1994).

RyR1 mutations causing malignant hyperthermia indicate functionally important locations of the Ca^{2+} release channel. In addition to modifying the response to chemical agonists (Otsu *et al.* 1994; Tong *et al.* 1997) they might influence the physiological interaction between the ryanodine and DHP receptors which could show up in alterations of Ca^{2+} conductance or of Ca^{2+} release. The voltage of half-maximal Ca^{2+} conductance and the maximal conductance per linear capacitance were not significantly different, but the steepness of the Ca^{2+} conductance activation curve was lowered. A similar change in voltage sensitivity is also evident from the current–voltage relations shown by Gallant *et al.* (1996). This may indicate a mild alteration in

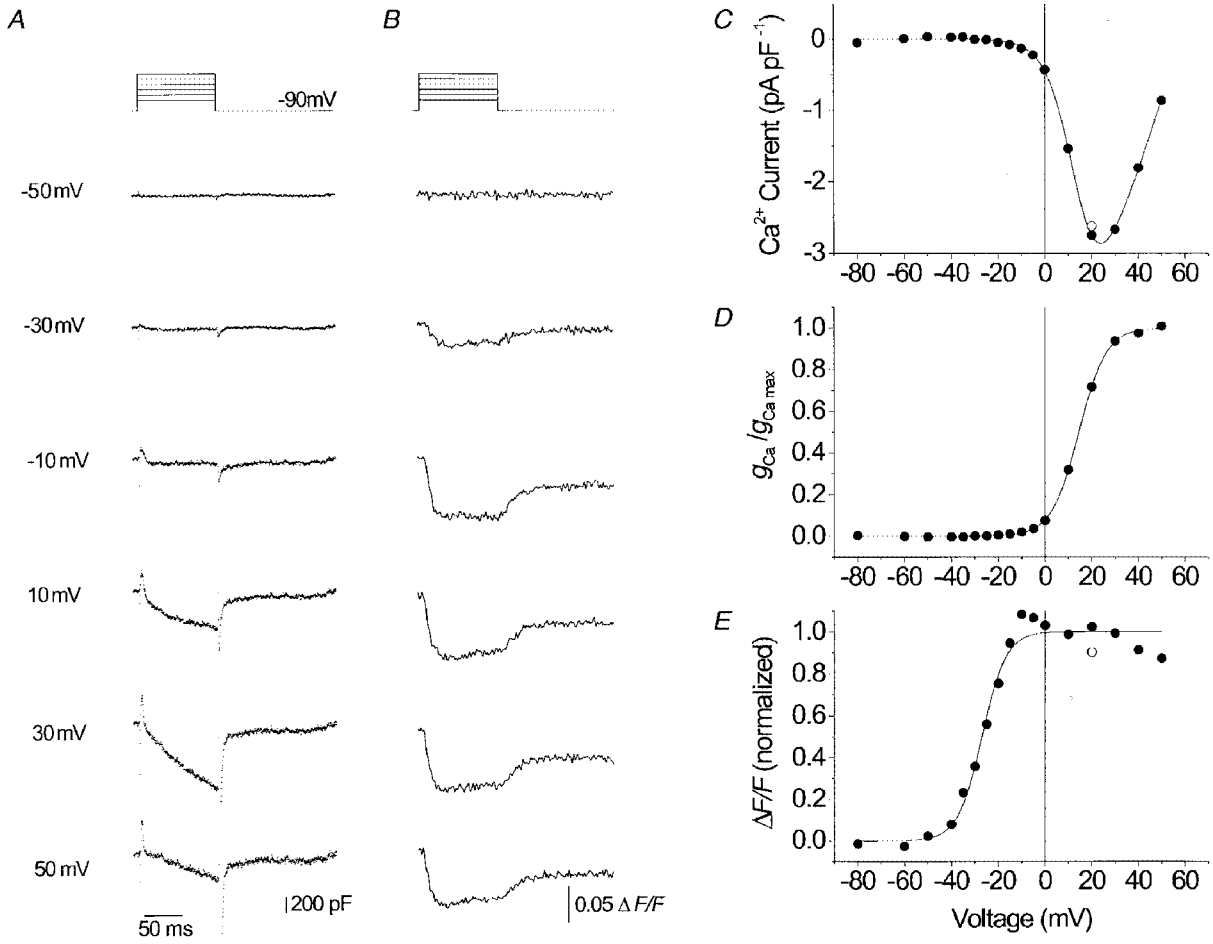

Figure 3. Ca^{2+} current and Ca^{2+} transients in an MHS myotube

L-type Ca^{2+} inward currents (*A*) and fluorescence signals (*B*) recorded at voltage-clamp steps from −90 mV to values between −50 and +50 mV. *C*, current–voltage relation. *D*, voltage dependence of Ca^{2+} conductance activation. *E*, voltage dependence of activation of the Ca^{2+} signal. Resting [Ca^{2+}]: 56 nM, Δ[Ca^{2+}] at +20 mV: 22 nM. Best fit parameters, current: $g_{Ca,max} = 99·2$ pS pF^{-1}, $V_{Ca} = 58·6$ mV, $V_{½} = 14·5$ mV, $k = 5·9$ mV. Fluorescence: $V_{½} = -27·0$ mV, $k = 5·2$ mV.

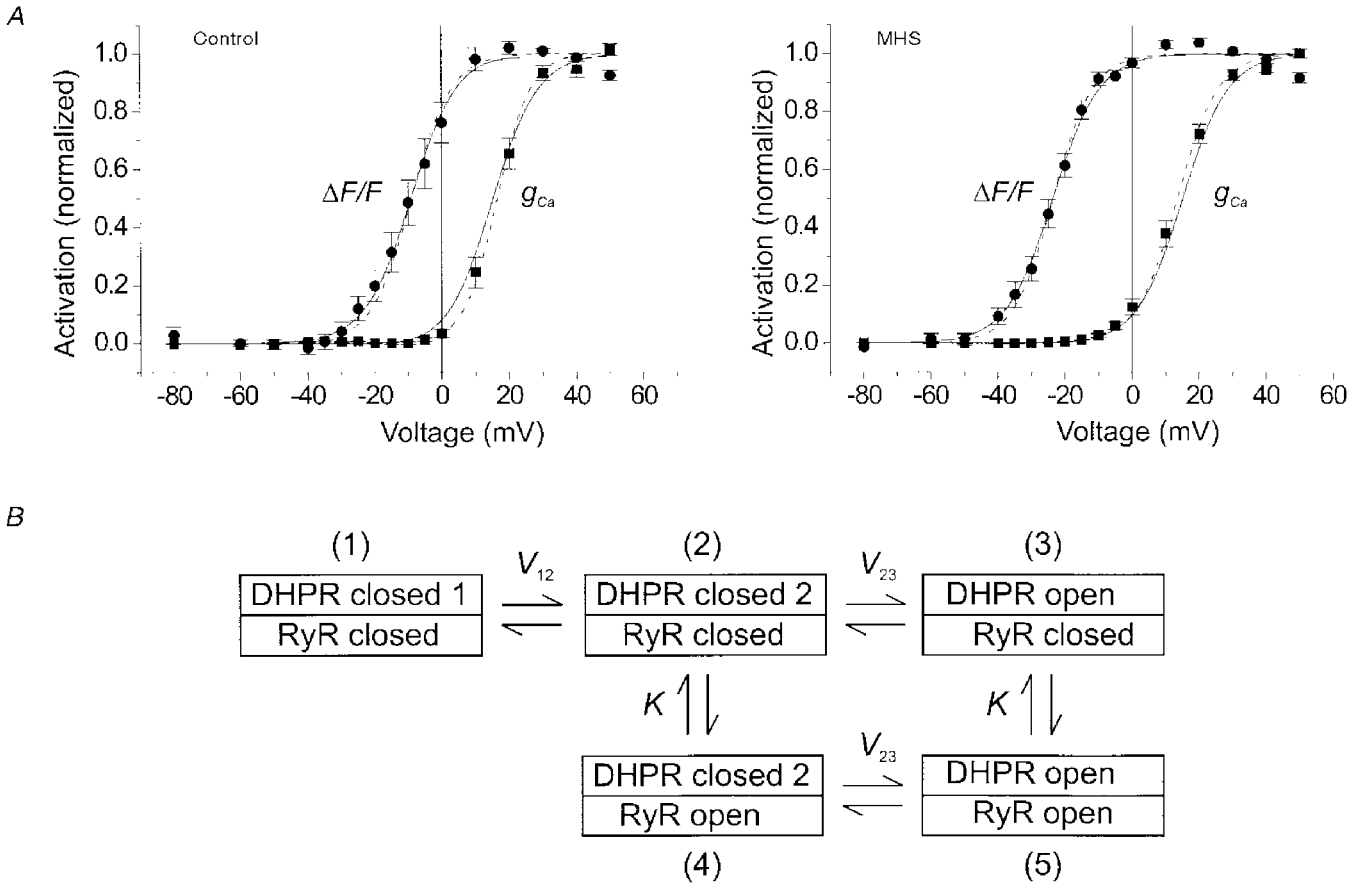

Figure 4. Voltage dependence of Ca^{2+} conductance and Ca^{2+} release in MHS and control myotubes

A, Ca^{2+} conductance (■) and Ca^{2+} release data (●) from experiments on control (left) and MHS myotubes (right) plotted as a function of test voltage. The main effect in MHS was a left-shift of the activation curve for Ca^{2+} release. The averaged best fit parameter values of individual fits by eqns (1) and (2) were as follows. Control ($n = 9$): $g_{Ca,max} = 66{\cdot}2 \pm 10{\cdot}5$ pS pF^{-1}, $V_{Ca} = 52{\cdot}2 \pm 3{\cdot}2$ mV, $V_{½} = 16{\cdot}5 \pm 1{\cdot}3$ mV, $k = 4{\cdot}9 \pm 0{\cdot}4$ mV. Fluorescence: $V_{½} = -9{\cdot}0 \pm 2{\cdot}4$ mV, $k = 6{\cdot}0 \pm 0{\cdot}4$ mV. MHS ($n = 19$): $g_{Ca,max} = 85{\cdot}0 \pm 11{\cdot}7$ pS pF^{-1}, $V_{Ca} = 53{\cdot}0 \pm 1{\cdot}8$ mV, $V_{½} = 13{\cdot}5 \pm 1{\cdot}2$ mV, $k = 6{\cdot}1 \pm 0{\cdot}2$ mV. Fluorescence: $V_{½} = -23{\cdot}5 \pm 1{\cdot}2$ mV, $k = 6{\cdot}0 \pm 0{\cdot}4$ mV. Dashed curves were drawn using these parameter values. Maximal inward current, maximal inward current density and voltage of maximal inward current were not significantly different: -357 ± 58 pA, $-2{\cdot}14 \pm 0{\cdot}27$ pA pF^{-1} and $21{\cdot}7 \pm 1{\cdot}1$ mV in the MHS group *versus* -347 ± 86 pA, $-1{\cdot}62 \pm 0{\cdot}36$ pA pF^{-1} and $23{\cdot}7 \pm 1{\cdot}3$ mV, respectively, in the control group. The same was true for cell capacitance, series resistance, g_{leak} and V_{leak}: 189 ± 21 pF, $11{\cdot}3 \pm 1{\cdot}9$ MΩ, $1{\cdot}85 \pm 0{\cdot}52$ nS and $-2{\cdot}3 \pm 5{\cdot}9$ mV for MHS *versus* 216 ± 33 pF, $12{\cdot}9 \pm 3{\cdot}2$ MΩ, $1{\cdot}68 \pm 0{\cdot}50$ nS and $9{\cdot}5 \pm 10{\cdot}7$ mV, respectively, for the controls. The means include data from experiments with a slightly different internal solution (fluo-3 instead of fura-2 or no ATP and creatine phosphate). When only the experiments with standard internal solution (see Methods) and with fura-2 were used, very similar results were obtained: $V_{½} = 13{\cdot}8 \pm 1{\cdot}9$ mV and $k = 6{\cdot}0 \pm 0{\cdot}3$ mV (MHS, $n = 7$) *versus* $V_{½} = 16{\cdot}8 \pm 3{\cdot}0$ mV and $k = 4{\cdot}5 \pm 0{\cdot}4$ mV (control, $n = 4$). The corresponding parameters for Ca^{2+} release were $V_{½} = -20{\cdot}9 \pm 1{\cdot}5$ mV and $k = 5{\cdot}4 \pm 0{\cdot}5$ mV (MHS) *versus* $V_{½} = -7{\cdot}8 \pm 2{\cdot}8$ mV and $k = 5{\cdot}6 \pm 0{\cdot}7$. This group allowed absolute estimates of resting $[Ca^{2+}]$ and $\Delta[Ca^{2+}]$ (determined at +20 mV; note small amplitudes due to high [EGTA]). The values showed considerable scattering and no significant difference: 110 ± 40 nM and 23 ± 4 nM (MHS) *versus* 51 ± 18 nM and 14 ± 4 nM (control), respectively. *B*, reaction scheme for coupled DHPR–RyR gating. The model assumes three states of the L-type Ca^{2+} channel: resting (DHPR closed 1), pre-active (DHPR closed 2) and open (DHPR open) with voltage-dependent transitions. The ryanodine receptor is either shut (RyR closed) or open (RyR open). When the L-type channel is in the resting state (1) the ryanodine receptor is assumed to have a negligible open probability. The equilibrium constants of the ryanodine receptor gating reactions associated with the pre-active and the open configuration of the L-type channel are assumed to be identical (K). The model was used to fit the data in *A* (continuous curves). A simultaneous fit to control and MHS data was carried out resulting in the following set of parameter values: $V_{12} = 22{\cdot}6$ mV, $V_{23} = 15{\cdot}0$ mV, $k_{12} = 7{\cdot}0$ mV, $k_{23} = 6{\cdot}9$ mV, $K = 0{\cdot}0014$ (MHS), $K = 0{\cdot}011$ (control). Note that small K values mean that the equilibrium is largely on the side of opening. The result shows that a change in K alone can explain the selective shift of $V_{½}$ for Ca^{2+} release to a more negative value.

retrograde transmission from RyR1 to the DHP receptor (Fleig *et al.* 1996; Nakai *et al.* 1996; Grabner *et al.* 1999).

The selective shift of the activation curve for Ca^{2+} release by about 15 mV that we describe here fits well with observations by Gallant and co-workers on altered threshold concentrations of potassium for contractile activation in adult porcine muscle (Gallant & Donaldson, 1989; Gallant & Lentz, 1992). Furthermore, our experiments on myotubes show that the lowering of rheobase voltage for contractile activation from −6·9 to −22·6 mV reported by Gallant & Jordan (1996) can in fact be attributed to modified characteristics of voltage activation of Ca^{2+} release.

One may wonder how the voltage dependence of Ca^{2+} release can be changed without a corresponding change in the voltage dependence of L-type Ca^{2+} conductance if release and conductance activation are subsequent events caused by the same voltage sensor molecules (Garcia *et al.* 1994). The scheme in Fig. 4*B* (see figure legend for details) shows one possible explanation. In this five-state model, states three and five contribute to Ca^{2+} conductance while states four and five generate Ca^{2+} release. Equations (3) and (4) describe the probabilities of the corresponding state occupancies as functions of voltage:

$$P_{(3\,\mathrm{or}\,5)}(V) = P_3(V) + P_5(V) = \frac{1}{1 + \exp((V_{23} - V)/k_{23})\left(1 + \frac{K\exp((V_{12} - V)/k_{12})}{1 + K}\right)} \quad (3)$$

and

$$P_{(4\,\mathrm{or}\,5)}(V) = P_4(V) + P_5(V) = \frac{1}{1 + K + \frac{K\exp((V_{12} - V)/k_{12})}{1 + \exp((V - V_{23})/k_{23})}}, \quad (4)$$

where V_{12} and V_{23} are the voltages for 1:1 distribution and k_{12}, k_{23} the voltage sensitivity constants for the 1–2 transitions and 2–3 transitions, respectively. K is the equilibrium constant for the RyR1 open–closed reaction (vertical transitions).

This model predicts strong changes in the voltage for half-maximal activation of Ca^{2+} release when changing the voltage-independent equilibrium constant K. The reaction described by K might be linked to the ligand-modulated gating of the isolated ryanodine receptor (e.g. Laver *et al.* 1997; Owen *et al.* 1997). The continuous curves in Fig. 4*A* show least-squares fits of eqns (3) and (4) to the experimental data. An eightfold decrease in K (causing a larger degree of opening at constant voltage) produced the selective negative shift of $V_{½}$ of Ca^{2+} release. Thus, despite the fact that Ca^{2+} current and Ca^{2+} release activation have a voltage-dependent step in common (1–2 transition), only the voltage dependence of Ca^{2+} release is changed by varying the single voltage-independent parameter K. The model also shows that a change causing the observed effect may be completely independent of the actual mechanism that couples RyR1 to the voltage sensor. The mutation may, therefore, be far from the coupling region.

In summary, our measurements showed a selective shift in the voltage dependence of Ca^{2+} release activation to more negative potentials in porcine MHS myotubes. Thus, Arg615Cys does not only promote ligand-induced Ca^{2+} release but also the depolarization-induced release controlled by the DHP receptor voltage sensor. A simple model shows that one does not have to postulate a change in interaction domains of the ryanodine receptor with the DHP receptor nor two different forms of DHP receptors (inward-current generating and Ca^{2+} release activating) to explain these results.

Baylor, S. M., Chandler, W. K. & Marshall, M. W. (1983). Sarcoplasmic reticulum calcium release in frog skeletal muscle fibres estimated from Arsenazo III calcium transients. *Journal of Physiology* **344**, 625–666.

Baylor, S. M. & Hollingworth, S. (1998). Model of sarcomeric Ca^{2+} movements, including ATP Ca^{2+} binding and diffusion, during activation of frog skeletal muscle. *Journal of General Physiology* **112**, 297–316.

Brinkmeier, H., Seewald, M. J., Eichinger, H. M. & Rüdel, R. (1993). Culture conditions for the production of porcine myotubes and myoballs. *Journal of Animal Science* **71**, 1154–1160.

Brum, G., Rios, E. & Stefani, E. (1988). Effects of extracellular calcium on calcium movements of excitation–contraction coupling in frog skeletal muscle fibres. *Journal of Physiology* **398**, 441–473.

Dietze, B., Bertocchini, F., Barone, V., Struk, A., Sorrentino, V. & Melzer, W. (1998). Voltage-controlled Ca^{2+} release in normal and ryanodine receptor type 3 (RyR3)-deficient mouse myotubes. *Journal of Physiology* **513**, 3–9.

Fleig, A., Takeshima, H. & Penner, R. (1996). Absence of Ca^{2+} current facilitation in skeletal muscle of transgenic mice lacking the type 1 ryanodine receptor. *Journal of Physiology* **496**, 339–345.

Gallant, E. M., Balog, E. M. & Beam, K. G. (1996). Slow calcium current is not reduced in malignant hyperthermic porcine myotubes. *Muscle and Nerve* 19, 450–455.

Gallant, E. M. & Donaldson, S. K. (1989). Skeletal muscle excitation–contraction coupling. II. Plasmalemma voltage control of intact bundle contractile properties in normal and malignant hyperthermic muscles. *Pflügers Archiv* **414**, 24–30.

Gallant, E. M. & Jordan, R. C. (1996). Porcine malignant hyperthermia: genotype and contractile threshold of immature muscles. *Muscle and Nerve* **19**, 68–73.

Gallant, E. M. & Lentz, L. R. (1992). Excitation–contraction coupling in pigs heterozygous for malignant hyperthermia. *American Journal of Physiology* **262**, C422–426.

Garcia, J. & Beam, K. G. (1994). Measurement of calcium transients and slow calcium current in myotubes. *Journal of General Physiology* **103**, 107–123.

Garcia, J., Tanabe, T. & Beam, K. G. (1994). Relationship of calcium transients to calcium currents and charge movements in myotubes expressing skeletal and cardiac dihydropyridine receptors. *Journal of General Physiology* **103**, 125–147.

Grabner, M., Dirksen, R. T., Suda, N. & Beam, K. G. (1999). The II-III loop of the skeletal muscle dihydropyridine receptor is responsible for the bi-directional coupling with the ryanodine receptor. *Journal of Biological Chemistry* **274**, 21913–21919.

Iaizzo, P. A. & Lehmann-Horn, F. (1989). The *in vitro* determination of susceptibility to malignant hyperthermia. *Muscle and Nerve* **12**, 184–190.

Jurkat-Rott, K., McCarthy, T. & Lehmann-Horn, F. (2000). Genetics and pathogenesis of malignant hyperthermia. *Muscle and Nerve* **23**, 4–17.

Klein, M. G., Simon, B. J., Szücs, G. & Schneider, M. F. (1988). Simultaneous recording of calcium transients in skeletal muscle using high- and low-affinity calcium indicators. *Biophysical Journal* **53**, 971–988.

Laver, D. R., Owen, V. J., Junankar, P. R., Taske, N. L., Dulhunty, A. F. & Lamb, G. D. (1997). Reduced inhibitory effect of Mg^{2+} on ryanodine receptor-Ca^{2+} release channels in malignant hyperthermia. *Biophysical Journal* **73**, 1913–1924.

MacLennan, D. H. & Phillips, M. S. (1992). Malignant hyperthermia. *Science* **256**, 789–794.

Melzer, W., Herrmann-Frank, A. & Lüttgau, H. C. (1995). The role of Ca^{2+} ions in excitation–contraction coupling of skeletal muscle fibres. *Biochimica et Biophysica Acta* **1241**, 59–116.

Melzer, W., Rios, E. & Schneider, M. F. (1987). A general procedure for determining the rate of calcium release from the sarcoplasmic reticulum in skeletal muscle fibres. *Biophysical Journal* **51**, 849–863.

Mickelson, J. R. & Louis, C. F. (1996). Malignant hyperthermia: excitation–contraction coupling, Ca^{2+} release channel, and cell Ca^{2+} regulation defects. *Physiological Reviews* **76**, 537–592.

Nakai, J., Dirksen, R. T., Nguyen, H. T., Pessah, I. N., Beam, K. G. & Allen, P. D. (1996). Enhanced dihydropyridine receptor channel activity in the presence of ryanodine receptor. *Nature* **380**, 72–75.

Otsu, K., Nishida, K., Kimura, Y., Kuzuya, T., Hori, M., Kamada, T. & Tada, M. (1994). The point mutation Arg615→Cys in the Ca^{2+} release channel of skeletal sarcoplasmic reticulum is responsible for hypersensitivity to caffeine and halothane in malignant hyperthermia. *Journal of Biological Chemistry* **269**, 9413–9415.

Owen, V. J., Taske, N. L. & Lamb, G. D. (1997). Reduced Mg^{2+} inhibition of Ca^{2+} release in muscle fibers of pigs susceptible to malignant hyperthermia. *American Journal of Physiology* **272**, C203–211.

Shirokova, N., Garcia, J., Pizarro, G. & Rios, E. (1996). Ca^{2+} release from the sarcoplasmic reticulum compared in amphibian and mammalian skeletal muscle. *Journal of General Physiology* **107**, 1–18.

Smith, P. D., Liesegang, G. W., Berger, R. L., Czerlinski, G. & Podolsky, R. J. (1984). A stopped-flow investigation of calcium ion binding by ethylene glycol bis(beta-aminoethyl ether)-*N,N'*-tetra-acetic acid. *Analytical Biochemistry* **143**, 188–195.

Strube, C., Beurg, M., Powers, P. A., Gregg, R. G. & Coronado, R. (1996). Reduced Ca^{2+} current, charge movement, and absence of Ca^{2+} transients in skeletal muscle deficient in dihydropyridine receptor beta 1 subunit. *Biophysical Journal* **71**, 2531–2543.

Tong, J., Oyamada, H., Demaurex, N., Grinstein, S., McCarthy, T. V. & MacLennan, D. H. (1997). Caffeine and halothane sensitivity of intracellular Ca^{2+} release is altered by 15 calcium release channel (ryanodine receptor) mutations associated with malignant hyperthermia and/or central core disease. *Journal of Biological Chemistry* **272**, 26332–26339.

Acknowledgements

We thank Drs W. Erhardt, H. Brinkmeier and R. Rüdel for support, stimulating discussions and the use of laboratory equipment, Mrs M. Rudolf-Dauner, Mrs S. Schäfer and Mr E. Schoch for expert technical help and Dr A. Struk and Mr R. P. Schuhmeier for providing calculation software. The project was supported by the IZKF-Ulm and by grants of the European Community (ERB-FMRX-CT96-0032) and the Deutsche Forschungsgemeinschaft (Me-713/10-1/2) to W.M.

Corresponding author

W. Melzer: Department of Applied Physiology, University of Ulm, Albert-Einstein-Allee 11, D-89069 Ulm, Germany.

Email: werner.melzer@medizin.uni-ulm.de